Biometals (2011) 24:1153–1168
DOI 10.1007/s10534-011-9474-x

Cyto- and genotoxicity of a vanadyl(IV) complex with oxodiacetate in human colon adenocarcinoma (Caco-2) cells: potential use in cancer therapy

Ana L. Di Virgilio · Josefina Rivadeneira · Cecilia I. Muglia · Miguel A. Reigosa · Nataliya Butenko · Isabel Cavaco · Susana B. Etcheverry

Received: 16 May 2011 / Accepted: 17 June 2011 / Published online: 14 July 2011

Abstract The complex of vanadyl(IV) cation with oxodiacetate, VO(oda) caused an inhibitory effect on the proliferation of the human colon adenocarcinoma cell line Caco-2 in the range of 25–100 μM ($P < 0.001$). This inhibition was partially reversed by scavengers of free radicals. The difference in cell proliferation in the presence and the absence of scavengers was statistically significant in the range of 50–100 μM ($P < 0.05$). VO(oda) altered lysosomal and mitochondria metabolisms (neutral red and MTT bioassays) in a dose–response manner from 10 μM ($P < 0.001$). Morphological studies showed important transformations that correlated with the disassembly of actin filaments and a decrease in the number of cells in a dose response manner. Moreover, VO(oda) caused statistically significant genotoxic effects on Caco-2 cells in the low range of concentration (5–25 μM) (Comet assay). Increment in the oxidative stress and a decrease in the GSH level are the main cytotoxic mechanisms of VO(oda). These effects were partially reversed by scavengers of free radicals in the range of 50–100 μM ($P < 0.05$). Besides, VO(oda) interacted with plasmidic DNA causing single and double strand cleavage, probably through the action of free radical species. Altogether, these results suggest that VO(oda) is a good candidate to be evaluated for alternative therapeutics in cancer treatment.

Keywords Vanadyl(IV) cation · Multidentate ligands · Cytotoxicity · Genotoxicity · Caco-2 tumoral cells

A. L. Di Virgilio · J. Rivadeneira · C. I. Muglia · S. B. Etcheverry (✉)
Cátedra de Bioquímica Patológica, Facultad de Ciencias Exactas, UNLP, 47 y 115 (1900), La Plata, Argentina
e-mail: etcheverry@biol.unlp.edu.ar

J. Rivadeneira · S. B. Etcheverry
CEQUINOR (CONICET-UNLP), Facultad de Ciencias Exactas, UNLP, La Plata, Argentina

M. A. Reigosa
Instituto Multidisciplinario de Biología Celular (IMBICE), 526 y Cno. Gral. Belgrano, La Plata, Argentina

N. Butenko · I. Cavaco
Departamento de Química, Bioquímica e Farmácia, Universidade do Algarve, Campus de Gambelas, 8005-139 Faro, Portugal

N. Butenko · I. Cavaco
Centro de Química Estrutural, Instituto Superior Técnico, TU Lisbon, Av Rovisco Pais, 1049-001 Lisbon, Portugal

Introduction

A variety of vanadium compounds have been synthesized so far in an effort to optimize the antitumoral effects of this metal (Aubrecht et al. 1999; Cortizo et al. 2001; Djordjevic 1995). In particular, vanadium antineoplastic activity has been demonstrated both in vivo and in vitro (Narla et al. 2001; Molinuevo et al.

2004; Molinuelo et al. 2008; Samanta et al. 2008; Kostova 2009). In this aspect, the chemical and biochemical characteristics of ligands play a major role.

In aqueous media, strong chelating ligands are very important because they display the ability of trapping different metal species (Harding and Moksdi 2000). This process becomes particularly significant in living systems, where different metals are acquired, transported and stored mostly by low-molecular-weight compounds involving multidentate oxygen donors from carboxylate, hydroxamate and catecholate ligands (Lippard and Berg 1984; Costas et al. 2004). For vanadyl(IV) cation, complexation with organic ligands is crucial to maintain the solubility of the cation under physiological conditions and to increase its bioavailability (Etcheverry and Cortizo 1998).

Among the family of multidentate oxygen donor species, oda = oxodiacetate, $O(CH_2COO^-)_2$ holds an OOO donor group and can complex metal ions by forming chelate rings (Baggio et al. 2003). This ligand has been extensively used and several structures containing this anion in different environments have been obtained (Chao et al. 2003).

As it is mentioned above, vanadium compounds are very interesting from a pharmacological point of view due to their different therapeutics applications (Djordjevic 1995; Etcheverry and Cortizo 1998). Vanadium compounds can exert their antitumoral actions through different mechanisms such as: reduction of cellular growth rate (antiproliferative effect), cytotoxic and genotoxic actions that may be triggered by the increment of oxidative stress or through different interactions at DNA level.

It is known that some inorganic compounds display DNA cleavage activity and for this reason they are considered *inorganic nucleases* (Butenko et al. 2009). These compounds are relevant as possible therapeutic agents in cancer chemotherapy. The V^{IV}-complex vanadyl(acetylacetonate), $V^{IV}O(acac)_2$, has been proposed as a particularly efficient insulin-enhancing compound (Crans 2000). Besides, a recent study (Fu et al. 2008) has demonstrated its anticancer potential and mechanism of action in a human hepatoma cell line: $V^{IV}O(acac)_2$ blocked the cell cycle permanently at the G1 phase on HepG2 cells.

The aim of the present study is to extend our previous observations on the bioactivity of VO(oda) on tumoral cells, focusing the attention on its cytotoxic and genotoxic effects in the human colon adenocarcinoma cell line Caco-2.

Materials and methods

Materials

Tissue culture materials were purchased from Trading New Technologies (Buenos Aires, Argentina). Dulbecco's Modified Eagles Medium (DMEM), fetal bovine serum (FBS) from GBO Argentina SA (Buenos Aires, Argentina); trypsin–EDTA was provided by Gibco (Gaithersburg, MD, USA); Rhodamine 123, GSH, GSSG, neutral red (NR) and MTT were purchased from Sigma Chemical Co. (St. Louis, MO, USA). Dihydrorhodamine 123 (DHR) was from Molecular Probes (Eugene, OR, USA). Phalloidin was purchased from Invitrogen Corporation (Buenos Aires, Argentina). DAPI Vectashield mounting medium H1200 was purchased from Vector Laboratories, Burlingame, CA, USA. Plasmid DNA (pA1) used for gel electrophoresis experiments was purchased from Bluescribe, Strata-gene, UK.

Methods

Preparation of VO(oda) solutions

VO(oda) (97% purity determined by thermal analysis) was synthesized and characterized according to literature (Del Río et al. 2003).

Fresh stock solutions of the complex and the free ligand were prepared in distilled water at 100 mM and diluted according to the concentrations indicated in the legends of the figures.

Cell culture and incubations

Caco-2 human colon adenocarcinoma cell line was grown in DMEM containing 10% FBS, 100 IU/ml penicillin and 100 μg/ml streptomycin at 37°C in 5% CO_2 atmosphere.

Cells in a 75 cm^2 flask were grown until reach 70–80% of confluence. Then, the cells were subcultured using 0.1% trypsin–1 mM EDTA in a Ca^{2+}–Mg^{2+} free phosphate buffered saline (PBS). For experiments, cells were grown in multi-well plates. When cells reached the desired confluence, the

monolayers were washed with DMEM and were incubated under different conditions according to the experiments.

Cell proliferation: crystal violet assay

A mitogenic bioassay was carried out as described by Okajima et al. (1992) with some modifications. Briefly, cells were grown in 48 well plates. When cells reached 70% confluence, the monolayers were washed twice with serum-free DMEM and incubated with medium alone (basal) and different concentrations (10–100 μM) of the complex or the free ligand. Besides, incubations with a mixture of 50 μM of vitamin C and E and increasing concentrations of the complex were also carried out. Cells were pre-incubated with the scavengers of ROS during 2 h previous to the addition of different concentrations of the complex. Following pre-incubations, different concentrations of VO(oda) were added for 24 h at 37°C. After this treatment, the monolayers were washed with PBS and fixed with 5% glutaraldehyde/PBS at room temperature for 10 min. After that, they were stained with 0.5% crystal violet/25% methanol for 10 min. Then, the dye solution was discarded and the plate was washed with water and dried. The dye taken up by the cells was extracted using 0.5 ml/well 0.1 M glycine/HCl buffer, pH 3.0/30% methanol and transferred to test tubes. Absorbance was read at 540 nm after a convenient sample dilution.

NR assay

The NR accumulation assay was performed according to Borenfreund and Puerner (1984). Cells were plated in 96 well culture plates (2.5×10^4 cells/well). Cells were treated with different VO(oda) concentrations for 24 h at 37°C in 5% CO_2 in air. After treatment, the medium was replaced by one containing 100 μg/ml NR dye and cells were incubated for other 3 h. Then, NR medium was discarded, the cells were rinsed twice with warm (37°C) PBS (pH 7.4) to remove the non-incorporated dye, and 100 μl of 50% ethanol, 1% acetic acid solution was added to each well to fix the cells releasing the NR into solution. The plates were shaken for 10 min, and the absorbance of the solution in each well was measured in a Microplate Reader (7530, Cambridge technology, Inc, USA) at 540 nm, and compared with wells with untreated cells. Optical density was plotted as percentage of control.

MTT (methyl tetrazolium) assay

The MTT assay was based on a report previously described (Mosmann 1983). Briefly, cells were seeded in a 96-multiwell dish, allowed to attach for 24 h and treated with different VO(oda) concentrations for 24 h. After this treatment, the medium was changed and cells were incubated with 0.5 mg/ml MTT under normal culture conditions for 3 h. Cell viability was marked by the conversion of the tetrazolium salt MTT (3-(4,5-dimethylthiazol-2-yl)-2,5-diphenyl-tetrazolium-bromide) to a colored formazan by mitochondrial dehydrogenases. Color development was measured spectrophotometrically in a Microplate Reader (7530, Cambridge technology, Inc, USA) at 570 nm after cell lysis in DMSO (100 μl/well). Cell viability is shown graphically as percent of the control value.

Cell morphology

Cells were grown on glass coverslips and incubated under control conditions (without complex addition) or with different concentrations of VO(oda) in serum-free DMEM for 24 h. Then, the cells were fixed and stained with Giemsa (Cortizo et al. 2000; Etcheverry et al. 2007). Samples were observed under light microscopy.

Cytoskeleton actin determination

A fluorescence technique was used to visualize actin cytoskeleton filaments. Cells were grown on glass coverslips until a 70% of confluence; after that the cells were incubated for 24 h at 37°C with different concentrations of VO(oda). Then, the cells were fixed, permeabilized during 4 min at room temperature using absolute ethanol (cold at −20°C), washed with PBS and blocked with non-fat milk for 2 h. After washing, the cells were incubated with Phalloidin-FITC for 2 h. The samples were washed twice and mounted in slides. Labeled cells with green fluorescence were observed using a fluorescence microscope.

Determination of reactive oxygen species (ROS) production

The possible VO(oda)-induced oxidative stress in the Caco-2 cells was evaluated by measurement of intracellular production of ROS after incubation of the cell monolayers with different concentrations of the complex during 4 h at 37°C. ROS generation was determined by oxidation of DHR-123 to rhodamine by spectrofluorescence as we have previously described (Cortizo et al. 2000). A mixture of 50 μM of vitamin C and E was used to evaluate the role of the oxidative stress in the complex cytotoxicity under similar concentrations and incubation time to those employed in the crystal violet assay.

Fluorometric determination of GSH and GSSG cellular levels

GSH and GSSG levels were determined in culture as follows. Confluent Caco-2 monolayers from 24 well dishes were incubated with different doses of VO(oda) for 24 h at 37°C. Then, the monolayers were washed with PBS and harvested by incubating with 250 ml Triton 0.1% for 30 min. For GSH determination, 100 ml aliquots were mixed with 1.8 ml of ice cold phosphate buffer (Na_2HPO_4 0.1 M–EDTA 0.005 M pH 8) and 100 ml *o*-phthaldialdehyde (0.1% in methanol) as it was described by Hissin and Hilf (1996). For the determination of GSSG, 100 ml aliquots were mixed with 1.8 ml NaOH 0.1 M and *o*-phthaldialdehyde as before. Previously, to avoid GSH oxidation the cellular extracts for GSSG determination were incubated with 0.04 M of *N*-ethylmaleimide (NEM). Fluorescence at an emission wavelength of 420 nm was determined after excitation at 350 nm. Standard curves with different concentrations of GSH or GSSG were processed in parallel. Protein content in each cellular extract was quantified using Bradford assay (Bradford 1976). The ratio GSH/GSSG was calculated for all the experimental conditions.

Single cell gel electrophoresis (SCGE) assay

For detection of DNA strand breaks the SCGE ('Comet') assay was used in the alkaline version, based on the method of Singh et al. (1988) with minor modifications. Under alkaline conditions, DNA loops containing breaks loose supercoiling, unwind and are released from the nuclei and form a 'Comet-tail' by gel electrophoresis. For this experiment, 2×10^4 cells were seeded in a 12-well plate; 24 h later the cells were incubated with various concentrations of VO(oda). After treatment, cells were suspended in 80 μl of 0.5% low melting point agarose (pH 7.4) and immediately pipetted onto a frosted glass microscope slide precoated with a layer of 0.5% normal melting point agarose to promote a firm attachment of the second layer. After these layers had solidified at 4°C for 5–10 min, slides were immersed in ice-cold freshly prepared lysis solution (2.5 M NaCl, 10 mM Tris, 100 mM Na_2EDTA, 1% Triton X-100, 10% DMSO, pH 10) at darkness for 1 h (4°C) in order to lyse the cells, remove cellular proteins and to permit DNA unfolding. Immediately after, slides were put in a horizontal electrophoresis tank containing 1 mM Na_2EDTA, 0.3 M NaOH (pH 12.7) and then electrophoresis was performed for 30 min at 25 V (4°C). Afterwards, slides were neutralised with a solution comprising 0.4 M Tris–HCl (pH 7.5) and stained with 4′,6-diamidino-2-phenylindole (DAPI; Vectashield mounting medium H1200). Analysis of the slides was performed in an Olympus BX50 fluorescence microscope equipped with appropriated filter combination with an X63 fluorescence objective. Cellular images were acquired with the Leica IM50 Image Manager (Imagic Bildverarbeitung AG). A total of 50 randomly captured cells per experimental point of each experiment was used to determine the tail moment (product of tail length by tail DNA percentage) using a free Comet scoring software (Comet Score version 1.5). Two parallel slides were performed for each experimental point. Independent experiments were repeated twice.

Agarose gel electrophoresis (AGE) of plasmid DNA

The plasmid DNA used for gel electrophoresis experiments was pA1, which consists of a full-length cDNA from Cytochrome P450 CYP3A1 inserted in the PBS plasmid vector (pBluescribe, Strata-gene, UK) and described elsewhere (Fisher et al. 1998). Plasmid DNA was amplified in *Escherichia coli* DH5a and purified using PureYieldTM Plasmid Midiprep System from Promega. Linear DNA was obtained by digestion of pA1 with *Hin*dIII and used as a reference in AGE. This reference was replaced,

in some experiments, with plasmid DNA digested with $VO(acac)_2$ in conditions known to produce the linearized DNA form (Butenko et al. 2009).

DNA concentration per nucleotide base pair (bp) was determined by UV absorption at 260 nm using the extinction coefficient of 13,200 M^{-1} cm^{-1} bp^{-1}.

A 200 μM mother solution of vanadium complex in deionized MilliQ water was freshly prepared for each experiment. Both complex and ligand are soluble in water.

DNA cleavage activity was evaluated by monitoring the conversion of supercoiled plasmid DNA (Sc) to nicked circular DNA (Nck) and linear DNA (Lin). Each reaction mixture was prepared by adding (in this order) 6 μl of water, 2 μl of 100 mM stock pH 7 buffer solution, 2 μl (0.2 μg) of supercoiled pA1 DNA and 10 μl of the aqueous solution of the complex. The buffers used in these experiments were MOPS/NaOH and phosphate/HNO_3. The final reaction volume was 20 μl and the final metal concentrations tested were 6, 12, 25, 50 and 100 μM. The final buffer concentration was 10 mM. When the reaction involved additional activating agents or radical scavengers, the initial volume of water was reduced to 4 μl, and 2 μl of a solution of the agent or scavenger were added before the metal complex. MPA and oxone were chosen as reducing and oxidizing activating agents, respectively. Several known OH radicals scavengers (Halliwell and Gutteridge 2007) sodium azide, DMSO and NaBz were used in the experiments. The final concentration was 200 μM for activating agents and 40 mM for scavengers. The control samples were prepared in the absence of metal complex. The sample containing hydrogen peroxide was prepared in the same way as those with activating agents or scavengers. The stock solution of ~1 mM hydrogen peroxide was freshly prepared from 30% H_2O_2, its concentration was measured spectrophotometrically ($\varepsilon_{230nm} = 74$ M^{-1} cm^{-1}) (Mueller et al. 1997).

Agarose powder (1.5 g) from Sigma-Aldrich was weighed following by adding 150 ml of 0.5× TBE (89 mM Tris–Borate, 1 mM EDTA, pH 8.3). The mixture was heated in a microwave oven (at middle power) until the agarose dissolved completely. 10 μl (10 μg/ml) of ethidium bromide were added upon cooling the mixture to approximately 65–70°C and poured on a clean casting plate with an appropriate comb and left for approximately 1 h at room temperature to solidify before using.

Samples were incubated for 1 h at 37°C, wrapped up in aluminium foil. After incubation, 5 μl of DNA loading buffer (0.25% bromophenol blue, 0.25% xylene cyanol, 30% glycerol in water) were added to each tube and the solution was loaded onto a 1% agarose gel in TBE buffer. Controls of non-incubated and of linearized plasmid were included in both extremes of a 16-well gel plate. The electrophoresis was carried out for 3 h at 100 V. Bands were visualized under UV light and photographed using an AlphaImager (Alpha Innotech).

Peak areas were measured by densitometry using AlphaEaseFC™ Software from Alpha Innotech. Peak areas for the Sc form were corrected using the factor 1.47 to account for its lower staining capacity by ethidium bromide (Bernadou et al. 1989) and used to calculate the percentage (%) of each form (Sc, Nck and Lin). The variability of results was estimated from the analysis replicate digestions using $VO(acac)_2$ as a reference standard metallonuclease (Butenko et al. 2009). Standard deviation for repeatability (s_r which measures the random variability within each experiment) for the peak area within the same gel was estimated as 0.8% for the Sc form and 6% for the Nck form. The s_r of the whole experimental procedure, including the preparation of solutions and incubation was 10, 6 and 3%, for the Sc, Nck and Lin forms, respectively. These values were estimated from analysis of variance (single factor ANOVA) of duplicates from 11 different runs. s_r for the peak area was estimated from duplicates of plasmid DNA (not incubated). s_r for the whole procedure was estimated from duplicates of samples incubated with metal complex (Butenko et al. 2009).

All experiments were done in duplicate, and the gel with best quality was presented as example.

Statistical analysis

For statistical analysis the following methods were used: One-way ANOVA followed by Newman–Keuls test for comparison of the differences and the Student t test for the comparison of two means. Results represent the mean ± SEM. All the results with $P < 0.05$ were considered statistically significant.

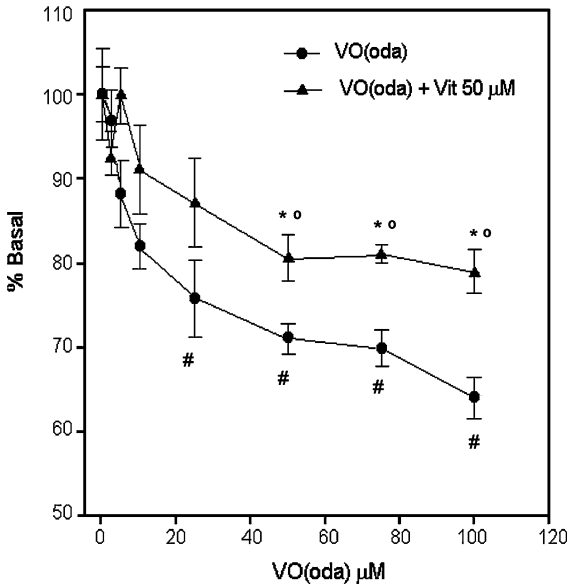

Fig. 1 Effect of VO(oda) on Caco-2 cell proliferation. Cells were incubated in serum-free DMEM without (basal) or with different concentrations of VO(oda) (2.5, 5, 10, 25, 50, 75 and 100 μM) at 37°C for 24 h. Results are expressed as % basal and represent the mean ± SEM ($n = 9$) *, # significant differences versus control, $P < 0.05$, ° significant differences in relation to the same concentration of the complex in absence of the mixture of vitamins, $P < 0.05$

Results

Effects of VO(oda) on Caco-2 cell proliferation

As can be observed in Fig. 1, VO(oda) exerted an inhibitory effect on Caco-2 cell proliferation in a dose response manner. This effect was statistically significant in relation to basal condition ($P < 0.001$) from 25 μM concentration. IC_{50} for the complex in Caco-2 cell line was ≫100 μM. Besides, the free ligand did not cause any effect on cell proliferation (data not shown).

The inhibition of Caco-2 proliferation was partially ameliorated by scavengers of free radicals as a mixture of vitamin C and E (50 μM). In the presence of vitamins, the deleterious effect of the complex can be seen at a concentration higher than in the absence of scavengers. The differences between these two conditions began to be statistically significant in the range of 50–100 μM ($P < 0.05$).

In this figure, the beneficial effect of 50 μM vitamin C plus vitamin E mixture can be seen.

To get a better understanding of the cytotoxic effect of the complex, we next studied its effects on the lysosomal and mitochondrial activity by means of NR uptake and MTT assay, respectively.

Effects of VO(oda) on lysosomal activity: NR assay

The metabolically active lysosomes display the capacity of uptake the NR dye. A loss of lysosomal activity, indicated by a decrease in the uptake of NR was observed when Caco-2 cells were exposed to VO(oda). The cytotoxic effects of VO(oda) in this cell line affects the functions of these organelles. This effect can be observed in Fig. 2.

As can be seen, the lower tested concentrations (2.5 and 5 μM) did not show any difference with the control condition (without complex addition). Nevertheless, at 10 μM a statistically significant decrease in the uptake of the dye by the lysosomes could be detected ($P < 0.001$). As the concentrations of VO(oda) increase, a marked cytotoxic effect could be observed in the 25–100 μM range ($P < 0.001$).

These results show that the alterations in the lysosomal activity begin at a concentration lower (10 μM) than the dose at which proliferation is statistically diminished (25 μM). At the latter concentration the lysosomal activity was reduced to 50% of the basal.

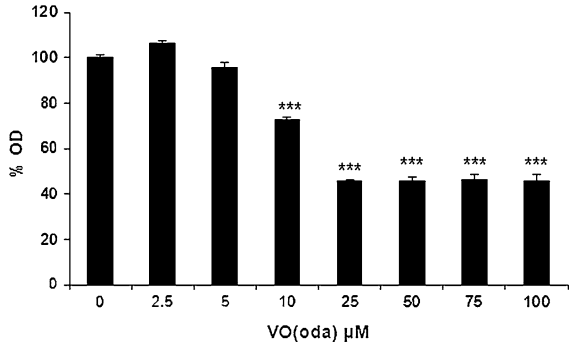

Fig. 2 NR uptake assay. Caco-2 cells were incubated with different doses of VO(oda) for 24 h at 37°C. After incubation, cell viability was determined by the uptake of NR. The dye taken up by the cells was extracted and the absorbance read at 540 nm. Results are expressed as % basal and represent the mean ± SEM ($n = 16$), ***$P < 0.001$

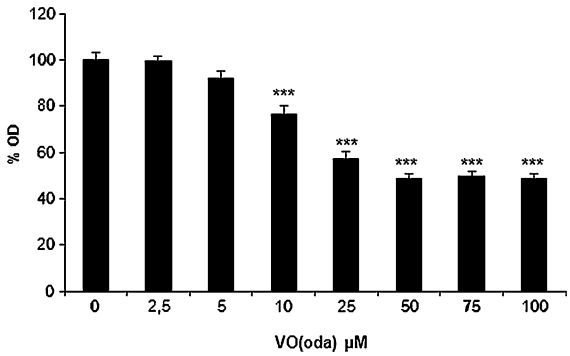

Fig. 3 MTT assay. Caco-2 cells were incubated with different doses of VO(oda) for 24 h at 37°C. After incubation, cell viability was determined by the conversion of the tetrazolium salt MTT to a colored formazan by mitochondrial dehydrogenases. Color development was measured at 570 nm after cell lysis in DMSO. Results are expressed as % basal and represent the mean ± SEM ($n = 16$), $^{***}P < 0.001$

Effects of VO(oda) on mitochondrial activity: MTT assay

Alteration in the energetic cell metabolism induced by VO(oda) measures the ability of the mitochondrial succinic dehydrogenases to reduce the methyl tetrazolium salt (MTT assay). The results presented in Fig. 3 show a decrease in the MTT dye reduction to an insoluble violet formazan product when Caco-2 cells were exposed to different complex concentrations (2.5–100 µM). In the presence of VO(oda), a significant decrease ($P < 0.001$) was observed in the absorbance for concentration values equal or higher than 10 µM. Cell metabolism inhibition in the 10–25 µM concentration range was lower (but still above 50%) than in the 50–100 µM range. At the higher tested concentrations the decreased in cell metabolism reached a plateau (ca. 45%). These results are in parallel with those of the NR uptake, suggesting that the cytotoxic actions of the complex affected the normal activity of mitochondria, contributing also in this way to the deleterious effect of VO(oda).

Morphological changes

Next we determined the effect of this complex on the morphology of Caco-2 cells. Morphological studies were carried out using Giemsa staining and light microscopy. In basal conditions, the cells displayed polygonal shape and big nuclei with numerous nucleoles. Cells present also numerous connections between each other (Fig. 4a). Upon incubation with the 25 and 100 µM complex concentrations, the nuclei showed different alterations in their form such as chromatine condensation and apoptotic bodies. Besides some membrane blebs could be seen especially at the highest dose (Fig. 4c). In addition, the cytoplasm of the cells also showed important transformations such as numerous irregular vacuoles and lost of neighboring connections. These changes increased with the doses and correlated with a decrease in number of cells per field (Fig. 4b, c). An important number of cells died and detached from the monolayers (Fig. 4c). Altogether, these are typical features of apoptosis, a process of cell death induced by the treatment with the complex.

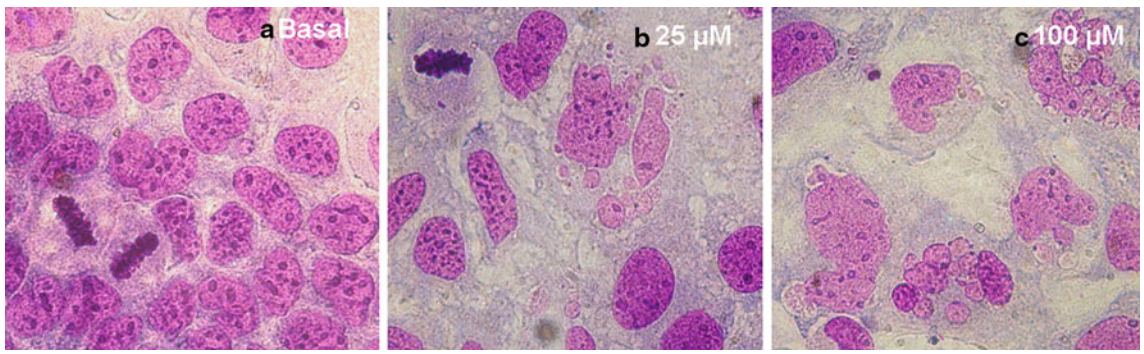

Fig. 4 Effect of VO(oda) on Caco-2 cells. Cells were incubated with VO(oda) for 24 h. Then, the cells were stained with Giemsa and observed by light microscopy (magnification 100×)

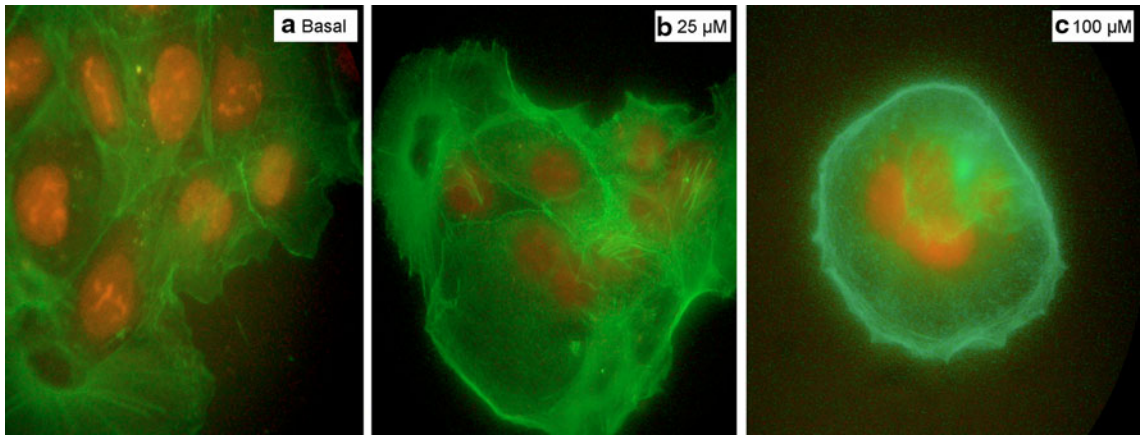

Fig. 5 Effect of VO(oda) on the actin cytoskeleton filaments of Caco-2 cells. Cells were incubated with different concentrations of VO(oda) for 24 h at 37°C. Then, the cells were stained with Phalloidin-FITC and observed by fluorescence microscopy (magnification 100×)

Interactions of VO(oda) with the actin filaments of cytoskeleton

The cytoskeleton network can be observed by the staining of the actin fibers with Phalloidin-FITC, a fluorescent probe with high affinity for the cytoskeleton. The disassembly of the network of actin microfilaments as a function of complex concentration can be observed in Fig. 5. Under normal conditions (Fig. 5a), the actin microfilaments were placed in the direction of the main axis of the cells. In the presence of the vanadium complex (25 and 100 μM), a rearrangement of the actin network could be observed. At 25 μM (Fig. 5b), VO(oda) caused a strong alteration in the actin arrangement but a higher effect was observed at 100 μM (Fig. 5c), a dose at which practically a total lost of the actin network could be seen. At this concentration, a complete disorganization was visualized with the fibers surrounding the nuclei of the cells and the shape of cells completely altered. All these actin changes were in parallel with serious disruption of cell shape and size. This result is in accordance with the morphological and the proliferation studies.

Genotoxicity: induction of DNA damage assessed by the Comet assay

The SCGE (Comet) assay was carried out in order to elucidate the genotoxic effect of VO(oda). In this assay three parameters are currently used: the Comet Length, the Tail Length and Tail Moment which are determined using a scoring software. The two first parameters are based on the migration of DNA. Most commonly, the distance of DNA migration is used to measure the extent of DNA damage. However, if DNA damage is relatively high, the tail increases in fluorescent staining intensity but not in length (Liao et al. 2009). Thus, it is also convenient to use the Tail Moment. This parameter is calculated as: Tail Length × DNA amount in the tail. DNA amount is determined through the intensity of fluorescence.

As can be seen from Fig. 6, the treatment with the complex produced an increment in the parameters of the standard alkaline Comet assay (Comet Length, Tail Length and Tail Moment). The genotoxic action of VO(oda) was already detectable at 5 μM ($P < 0.001$ for the Comet Length and Tail Length parameters). Besides, VO(oda) caused an increase of Tail Moment value in a concentration dependent fashion ($P < 0.01$ at 5 μM and $P < 0.001$ from 10 to 25 μM). The Comet assay detects DNA damage due to direct genotoxic impact of different agents or it can also correlate with DNA degradation due to necrosis or apoptosis. The two latter processes could introduce a false positive response due to cytotoxic events. Henderson et al. (1998) indicated that the maximum concentration of tested agent should produce viabilities >75% in order to avoid cytotoxicity-induced false positive responses in the study of genotoxic effects. In our study, the percentage of viable cells observed in the proliferation assay indicates the lack of overt cytotoxic effects in the range of concentrations within 2.5–10 μM, i.e. the

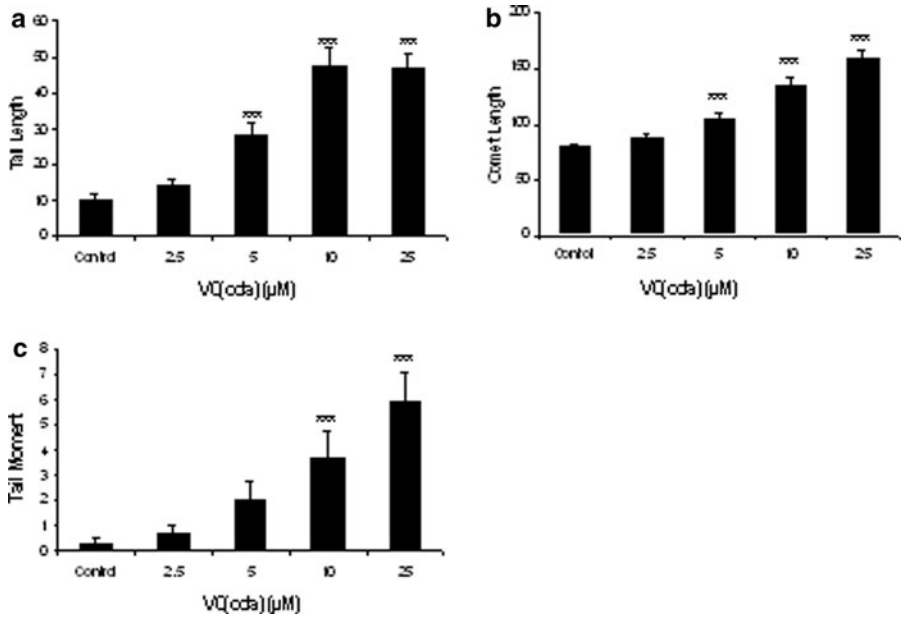

Fig. 6 SCGE (Comet assay). Induction of DNA damage by VO(oda) in Caco-2 cells was evaluated by **a** Tail Length, **b** Comet Length and **c** Tail Moment. After incubation with VO(oda) for 24 h, cells were lysed. After electrophoresis, nuclei were stained and analyzed. Results are expressed as mean ± SEM ($n = 150$), ***$P < 0.001$

viability remains above 75%. However, the DNA damage detected at higher VO(oda) concentrations (25 μM) may be due to secondary events; i.e. related to the cytotoxicity of VO(oda).

Mechanisms of the toxic effects

Oxidative stress

In order to get a deeper insight into the mechanisms underlying the cytotoxicity of VO(oda), we determined its effect on the oxidative stress using two parameters: the oxidation of dihydrorhodamine 123 to rhodamine (measured by spectrofluorometry) and the changes in the ratio of reduced glutathione (GSH) to oxidized glutathione (GSSG).

The complex produced a great increment in the levels of rhodamine in the range of 50–100 μM ($P < 0.001$) (see Fig. 7). Besides, the mixture of vitamins C and E, scavenger of free radicals, caused a decrease in the oxidative stress produced by VO(oda) in the range of 50–100 μM ($P < 0.05$).

Glutathione is the major antioxidant found in most mammalian tissues. Its oxidation to GSSG generates a redox buffer that protects cells from oxidative stress. Under oxidant conditions, the GSH/GSSG ratio diminishes. After treatment of Caco-2 tumoral cells with the complex, we found that GSH levels

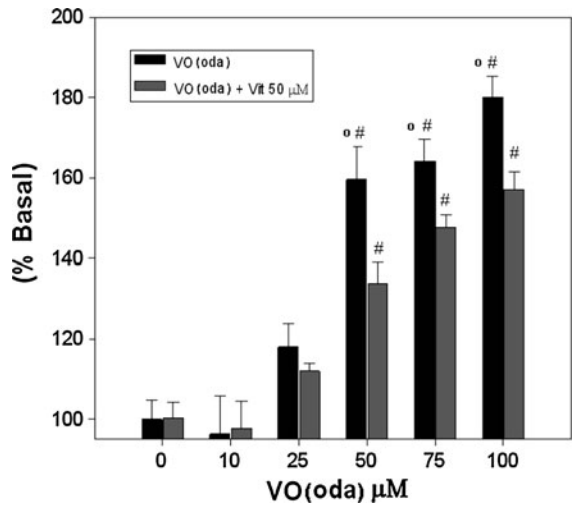

Fig. 7 Induction of ROS by VO(oda) in Caco-2 cells. Cells were incubated with growing concentrations of VO(oda) at 37°C for 24 h. ROS production in the cells was evaluated through the oxidation of DHR-123 to Rhodamine 123 (RH123). Results represent the mean ± SEM ($n = 6$), #significant differences versus control $P < 0.05$, °significant differences in relation to the same concentration of the complex in absence of the mixture of vitamins, $P < 0.05$

decreased in a dose dependant manner in the range of 50–500 μM ($P < 0.05$) (Fig. 8a). Moreover a decrease in the GSH/GSSG ratio was also observed for 100 and 500 μM ($P < 0.05$) (Fig. 8b).

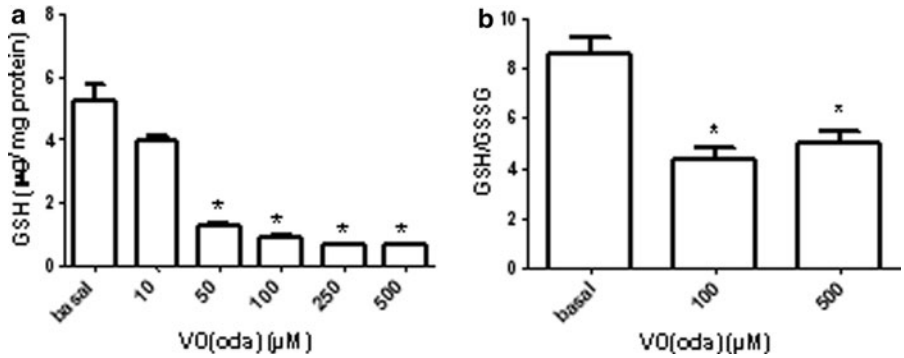

Fig. 8 **a** GSH level in Caco-2 cells in presence of different VO(oda) concentrations. Results are expressed as the mean ± SEM of three independent experiments, *significant differences versus basal, $P < 0.05$. **b** GSH/GSSG ratio in Caco-2 cells incubated with different concentrations of VO(oda). Results are expressed as the mean ± SEM of three independent experiments, *significant differences versus basal, $P < 0.05$

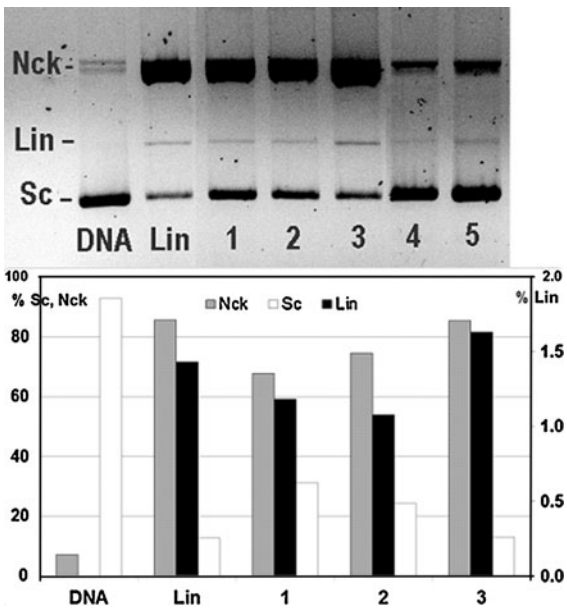

Fig. 9 AGE of plasmid DNA digested with VO(oda) with and without activating agents. The *graphic* shows percentages of Sc, Nck and linear forms, measured from the corresponding AGE bands. Controls for native DNA and for the linear form are represented as "DNA" and "Lin". *1* VO(oda), *2* VO(oda) + MPA, *3* VO(oda) + Oxone. VO(oda) concentration is 50μM (r.i. = 1.7), solutions are buffered at pH 7.0 with MOPS. *Error bars* were estimated as ±2 s for 95% confidence intervals

Effect of VO(oda) on plasmidic DNA: AGE

From Fig. 9 it is clear that VO(oda) cleaves DNA under relatively mild conditions (1 h digestion at 37°C). The intensities of the nicked (Nck) bands are much stronger than the supercoiled (Sc) bands in DNA samples digested with VO(oda). This indicates an extensive single-strand cleavage of DNA at relatively low ratios of metal:bp (1.7). Double-strand cleavage of DNA is also detected since a light band corresponding to the linear form is observed in all samples digested with VO(oda). The addition of mercaptopropionic acid (MPA) did not affect the activity of VO(oda) significantly, but increased it slightly. Addition of the strong oxidant oxone ($KHSO_5$) induced a further increase in the activity, observed by the stronger intensity of both the Nck and Lin bands.

It is known that the nature of the pH buffer may affect the observed nuclease activity, particularly when changing from organic to inorganic buffers (Butenko et al. 2009). In order to evaluate any effect of the buffer, parallel experiments with variable complex concentration were carried out at pH 7.0 under two different pH buffers, phosphate and MOPS (Fig. 10). In both cases, the extent of DNA cleavage is closely dependent with complex concentration. The activity of VO(oda) can be already observed starting from the most diluted sample—6 μM—in both buffers. Nevertheless, VO(oda) shows a higher activity under phosphate buffer than under MOPS.

The effect of three radical scavengers—sodium azide (NaN_3), dimethyl sulfoxide (DMSO) and sodium benzoate (NaBz)—is shown in Fig. 11. Under MOPS buffer it is clear that NaN_3 quenches the activity of VO(oda) much more strongly than DMSO and NaBz. Unlike NaBz and DMSO, NaN_3 may scavenge singlet oxygen species as well as hydroxyl radicals and other ROS. The fact that the reaction is

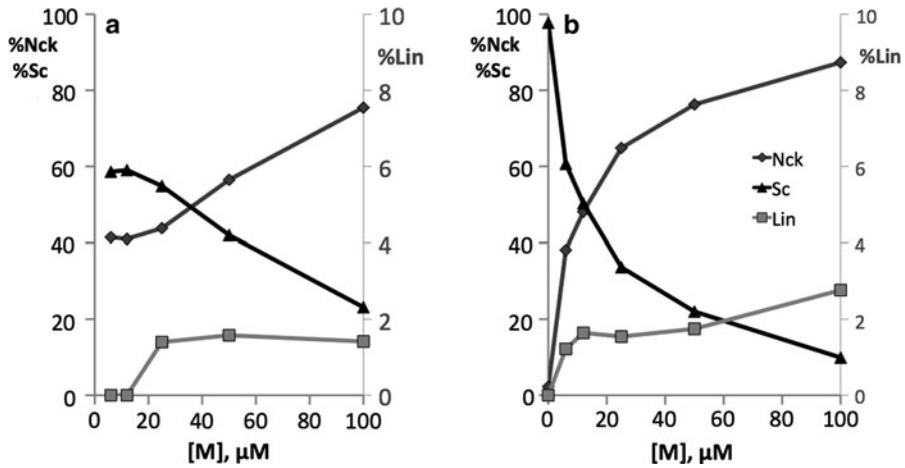

Fig. 10 Evolution of DNA degradation with increasing concentration of VO(oda). **a** Solutions buffered at pH 7.0 with MOPS, **b** solutions buffered at pH 7.0 with phosphate buffer

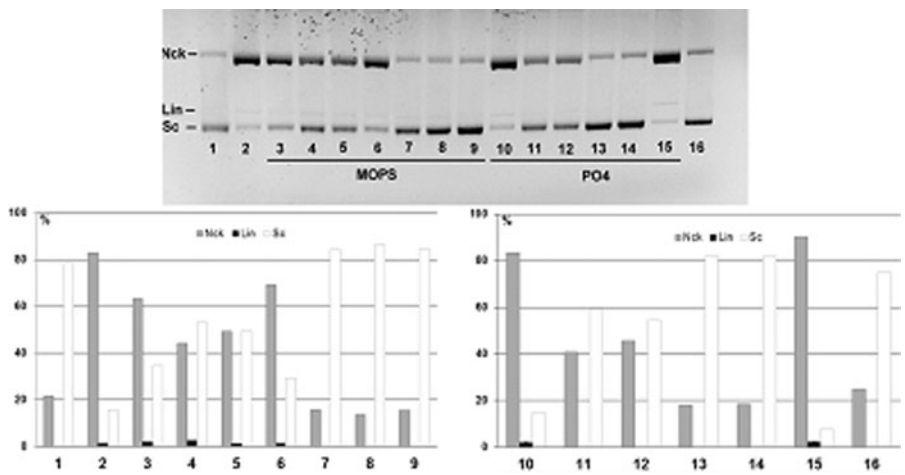

Fig. 11 DNA cleavage of VO(oda) with addition of radical scavengers: sodium azide, DMSO and sodium benzoate. *Samples 1, 16* controls of native DNA; *2, 15* controls of linearized DNA; *3* VO(oda); *4* VO(oda) + NaN_3; *5* VO(oda) + NaBz; *6* VO(oda) + DMSO; *7* NaN_3 control; *8* NaBz control; *9* DMSO control; *10* VO(oda); *11* VO(oda) + NaN_3; *12* VO(oda) + NaBz; *13* NaN_3 control; *14* NaBz control. *Samples 2, 10–15* were prepared under phosphate buffer; *3–9* under MOPS buffer. Final complex concentration was 100 μM

reduced more efficiently in the presence of NaN_3 than the other scavengers suggests that singlet oxygen may play a role in the activity of VO(oda) under MOPS buffer. It is interesting to note that some linearization of DNA was still observed in all samples, as if the quenching was only effective for the single-strand cleavage and not the double-strand one. This residual activity points to the possibility of another, non-radicalar mechanism, taking place.

Under phosphate buffer both NaN_3 and NaBz decrease the nuclease activity to the same extent, and no linearization is observed in samples containing radical scavengers. Some residual activity is still observed after the addition of the radical scavengers, though weaker than under MOPS buffer.

These results point to different mechanisms of DNA cleavage by VO(oda) in these buffers. It is possible that under phosphate buffer different species

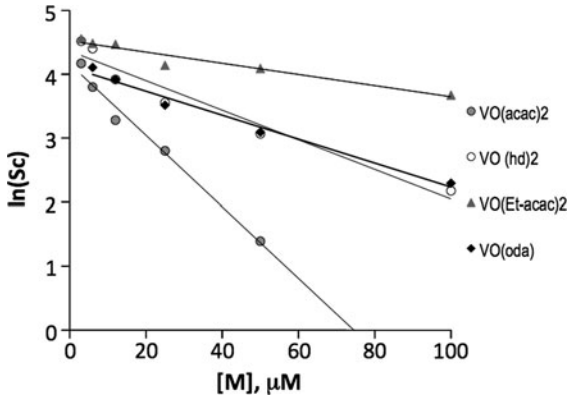

Fig. 12 Comparison of cleavage activity of VO(oda) with other vanadium nucleases: $VO(acac)_2$, $VO(hd)_2$ and $VO(Et\text{-}acac)_2$ (Butenko et al. 2009; Costa Pessoa et al. 2007; Cavaco et al. 2009). Cleavage efficiency is measured by the slope of the straight line of the logarithm of the percentage of Sc (log SC) with complex concentration

containing phosphate in the vanadium coordination sphere may form and induce a different mechanism for DNA cleavage.

Figure 12 compares the nuclease activity of VO(oda) under phosphate buffer with other active vanadyl complexes such as $VO(acac)_2$, $VO(hd)_2$ and $VO(Et\text{-}acac)_2$ previously tested in similar conditions (Butenko et al. 2009; Costa Pessoa et al. 2007; Cavaco et al. 2009) showing that VO(oda) is quite an efficient nuclease. It has a similar activity to $VO(hd)_2$, lower than the nuclease activity of $VO(acac)_2$ and higher than $VO(Et\text{-}acac)_2$.

Discussion

Recently, there has been an increasing interest in the antitumoral effects of vanadium derivatives (Aubrecht et al. 1999; Cortizo et al. 2001; Narla et al. 2001; Evangelou 2002; Hanauske et al. 1987; Holko et al. 2008; Klein et al. 2008). It has been previously demonstrated that vanadium compounds exert a reduction of tumoral growth both in vivo and in vitro model systems (Molinuevo et al. 2004; Kostova 2009; Bishayee et al. 1999; Barrio et al. 2003; Evangelou et al. 1997).

Vanadium complexes that belong to the group of non-platinum metal antitumor agents have shown to possess a wide spectrum of antineoplastic properties. These compounds appear to offer a different alternative for cancer chemotherapy which does not follow the mechanism of action of the platinum complexes (Farrell 1999).

As part of a research project devoted to the investigation of vanadium complexes with potential pharmacological applications, we have tested the antitumoral effects of a complex of vanadyl(IV) cation with a multidentate oxygen donor, oxodiacetate, in a model system of human colon adenocarcinoma Caco-2 cells in culture. In this paper, we have investigated the cyto- and genotoxic effects of VO(oda) and also we have tried to elucidate the putative mechanism of action underlying its effects. We have studied the effects of VO(oda) on cell proliferation, cell morphology and on the cytoskeleton actin fibers. We observed a deleterious effect of the complex on the proliferation of Caco-2 cells in culture (Fig. 1). This finding is in agreement with a previous paper reporting the inhibition of cell proliferation by the same vanadium(IV) complex in a rat osteosarcoma derived cell line (UMR106) (Rivadeneira et al. 2007). In both tumoral cell lines the inhibitory action of VO(oda) begun at 25 μM. The sensitivity of the rat osteosarcoma cells towards the complex seems to be slightly higher than the Caco-2 cells since at 100 μM there was ca 65% of surviving cells versus ca. 55% for the UMR106 cells.

The cytotoxic effects of VO(oda) on Caco-2 cells may be due to different causes such as the functional disruption of several organelles like the lysosomes and the mitochondria.

The metabolic activity of the lysosomes may be determined by the uptake of NR supravital dye. Viable cells will take up the dye, so any decrease in the uptake will serve as an indicator of cytotoxicity. On the other hand, the mitochondrial dehydrogenase enzyme activity can be measured through the determination of the reduction of MTT which is colored in its reduced form. After 24 h incubation with different concentrations of the complex, a reduction in these two important metabolic functions could be determined in Caco-2 cells in the 10–100 μM range (Figs. 2, 3). According to these results, the cytotoxic effects began at a lower concentration than the determined decrease in cell proliferation studies with the crystal violet assay. These results are in agreement with previous reports on the action of different vanadium species in several cell types. Decrease cell viability was induced by vanadyl sulphate in

tumorigenic and non carcinogenic cells (Holko et al. 2008), as well as the toxicity of vanadate solution in cardiomyocytes (Soares et al. 2008). Moreover, it has been also previously reported that vanadocenes blocked the cell division in human cancer cells by disrupting bipolar spindle formation. Vanadocene treatment caused an arrest at the G2/M phase of the cell cycle. This unique mechanism of anti-mitotic function warrants further development of vanadocene complexes as anti-cancer drugs (Navara et al. 2001). It has also been shown that vanadocene compounds induced apoptosis in human testicular cancer cell lines (Ghosh et al. 2000). It was also reported that the toxicity of vanadyl complexes on Caco-2 monolayer involved F-actin-related change of tight junction and impairment of microvilli. The toxicity was also related to elevated intracellular ROS and their cellular accumulation (Yang et al. 2004). VO(oda) has been shown to display a strong effect on the architecture of the actin cytoskeleton fibers which arrangement was affected in a dose response manner for the vanadyl complex (Fig. 5). The observed disruption of the actin fibres induced by VO(oda) may be related to toxic effects on the mitotic spindle in a way similar to that previously reported for vanadocenes. These changes also may be the cause of the observed apoptotic morphological alterations (Fig. 4) which were similar to those observed in the model of osteosarcoma cells and confirmed by flow cytometry studies (Rivadeneira et al. 2010). It has been reported that changes in actin fibers and cell-to-cell contact are involved in the antimetastatic potential of vanadium compounds (Dharwan et al. 1997; Luber et al. 2000).

In an attempt to elucidate the mechanism involved in the effects of VO(oda), we studied the relationship between the oxidative stress, GSH levels and the antiproliferative effect of VO(oda) in the tumoral cells. The results showed that GSH levels as well as the ratio GSH/GSSG (Fig. 8), which is a better marker of the GSH metabolism, decreased in parallel with the increment in the oxidative stress determined by the DHR123 oxidation (Fig. 7). Oxidative stress exerted on cells by other vanadium(IV) compounds has been previously reported (El-Naggara et al. 1998; Younes et al. 1991).

Indeed, this effect has been regarded as one of the major effects implicated in their anti tumorogenic activity, while a rise in GSH levels upon treatments has been observed in therapy resisting cells (Majumder et al. 2006).

On the other hand, it was observed a decrease in Caco-2 cell proliferation in the range of 50–100 μM (Fig. 1). This toxic effect could be ameliorated by the pre-incubation with a mixture of ROS scavengers (mixture of vitamin C and E) (Fig. 1), suggesting that the main mechanism involved in the VO(oda) cytotoxicity was the oxidative stress.

Vanadium compounds may also exert antiproliferative effects via interactions with DNA. It was previously reported that vanadocene complexes interact with DNA's nucleotide phosphate groups forming a labile outer sphere complex via a water group (Harding and Moksdi 2000; Harding et al. 1993; Kopf-Maier et al. 1981; Murray and Harding 1994; Toney et al. 1986). DNA cleavage in vivo and in vitro is also induced by a variety of vanadium compounds (Altamirano-Lozano et al. 1999; Lloyd et al. 1997; Rojas et al. 1996; Sakurai 1994; Sakurai et al. 1995; Sit et al. 1996). Several lines of evidence indicate that V(IV) and V(V) induce DNA cleavage through the production of ROS, especially hydroxyl radicals ($OH^{\bullet}$) generated in cells (Sakurai 1994).

Taking into consideration that genotoxicity is a process that can begin before the alterations at cytoplasm level could be detected; we investigated the effect of the complex at DNA level. Comet assay showed that VO(oda) induced alterations in the nuclei of the cells at 5 and 10 μM (Fig. 6), which indicated that the changes in DNA begun before any alteration in cell morphology, actin fibers, oxidative stress and cell number diminution could be observed.

The genotoxicity of VO(oda) was evaluated using the single cell gel electrophoresis (Comet assay). Vanadium has been considered an aneugen (any agent that affects cell division and the mitotic spindle apparatus resulting in the loss or gain of whole chromosomes). However, there is controversial information about the clastogenic effects of vanadium compounds (Rodríguez-Mercado et al. 2003). Our results showed a significant increase in three parameters evaluated with the Comet assay; this indicates that VO(oda) is able to induce DNA single and double-strand breaks and/or alkali-labile damage at very low doses (5 μM) (Fig. 6). Our results agree quite well with previous studies on the effects of vanadium compounds in different cell lines. Vanadium pentoxide produced a clear dose–response in

DNA migration in whole blood leukocytes and a significant positive effect only observed at higher concentrations in human lymphocyte cultures (Rojas et al. 1996). Moreover, vanadyl sulfate induced DNA damage in human normal lymphocytes and in HeLa cells (Wozniak and Blasiak 2004). These results point to the fact that this compound is genotoxic for normal and cancer cells. Interestingly, it has a higher genotoxic potential for the latter than for normal lymphocytes. Incubation of the cells with nitrone spin traps decreased the extent of DNA damage, which might follow from the production of free radicals by vanadyl sulfate (Wozniak and Blasiak 2004).

In order to get a deeper insight on the genotoxic action of VO(oda) at the DNA level, we have investigated its effect on plasmidic DNA. In comparison to some other vanadyl compounds such as $VO(acac)_2$, $VO(hd)_2$ and $VO(Et\text{-}acac)_2$. DNA degradation promoting by VO(oda) is relatively high. VO(oda) displays similar activity to $VO(hd)_2$, although it is still lower than the cleavage activity of $VO(acac)_2$ but, at the same time, much higher than the one of $VO(Et\text{-}acac)_2$ (Fig. 12). VO(oda) is quite active under the tested conditions since it interacted with plasmidic DNA at very low concentration (6 μM) (Fig. 10) in agreement with the results obtained by the Comet assay in the cells. The activity on plasmidic DNA is increased in the presence of strong oxidants (oxone, H_2O_2), but not in the presence of reductants (MPA) (Fig. 9). Besides, VO(oda) nuclease activity is quenched by radical scavengers (Fig. 11), suggesting a mechanism involving ROS. Nevertheless, a significant residual activity remains in the presence of scavengers, suggesting that a degree of DNA cleavage could be due to a parallel hydrolytic mechanism.

Conclusions

Altogether these results suggest that VO(oda) exerts its cytotoxic effects on human colon adenocarcinoma (Caco-2) cells through, at least in part, an increment in the oxidative stress and the alterations of actin cellular network. Besides, the deleterious action of VO(oda) also produced double and single DNA strand breaks.

The antiproliferative effects of VO(oda) in tumoral cell lines indicate that this complex is an interesting compound to be further evaluated in animal models of cancer since it may offer a different alternative for tumor chemotherapy.

Acknowledgments The authors would like to thank Prof. Dr. E.J. Baran for the preparation of VO(oda) complex and Prof. Dr. L. Bruzzone for the fluorometric measurements of DHR experiments. This work was supported by UNLP, CONICET (PIP 1125) and ANPCyT (PICT 2218), and the Erasmus Mundus Programme, EMQAL 2008-0095, for mobility funding. JR is a postdoctoral fellowship from CONICET, Argentina. ALDV, CIM and SBE are members of the Carrera del Investigador, CONICET, Argentina. MAR is a member of Carrera de Personal de Apoyo, CONICET, Argentina. NB is a doctoral student of the Erasmus Mundus External Cooperation Window—Lot 6. IC is Prof. of the Algarve University, Faro, Portugal.

Conflict of interest The authors declare that there are no conflicts of interest.

References

Altamirano-Lozano M, Valverde M, Alvarez-Barrera L, Molina B, Rojas E (1999) Reprotoxic and genotoxic studies of vanadium pentoxide (V2)O(5) in male mice. II. Effects in several mouse tissues. Teratog Carcinog Mutagen 19:243–255

Aubrecht J, Narla RK, Ghosh P, Stanek J, Uckun FM (1999) Molecular genotoxicity profiles of apoptosis-inducing vanadocene complexes. Toxicol Appl Pharmacol 154:228–235

Baggio R, Garland MT, Perec M (2003) A new polymeric phase of zinc (II)oxidiacetate. Acta Cryst C Cryst Struct Commun 59(1):30–32

Barrio DA, Williams PAM, Cortizo AM, Etcheverry SB (2003) Synthesis of a new vanadyl(IV) complex with trehalose (TreVO): insulin-mimetic activities in osteoblast-like cells in culture. J Biol Inorg Chem 8:459–468

Bernadou J, Pratviel G, Bennis F, Girardot M, Meunier B (1989) Potassium monopersulfate and a water-soluble manganese porphyrin complex, $[Mn(TMPyP)](OAc)_5$, as an efficient reagent for the oxidative cleavage of DNA. Biochemistry 28:7268–7275

Bishayee A, Roy S, Chatterjee M (1999) Characterization of selective induction and alteration of xenobiotic biotransforming enzymes by vanadium during diethylnitrosamine-induced chemical rat liver carcinogenesis. Oncol Res 11:41–53

Borenfreund E, Puerner JA (1984) A simple quantitative procedure using monolayer culture for toxicity assays. J Tissue Cult Methods 9:7–9

Bradford M (1976) A rapid and sensitive method for the quantitation of microgram quantities of protein utilizing the principle of protein-dye binding. Anal Biochem 72:249–254

Butenko N, Tomaz AI, Nouri O, Escribano E, Moreno V, Gama S, Ribeiro V, Telo JP, Costa Pessoa J, Cavaco I

(2009) DNA cleavage activity of VIVO(acac)$_2$ and derivatives. J Inorg Biochem 103:622–632

Cavaco I, Butenko N, Tomaz AI, Ribeiro V, Costa Pessoa J (2009) Studies on the mechanism of action of an efficient vanadium inorganic nuclease, VO(acac)$_2$. J Biol Inorg Chem 14:S183

Chao J, Xiang Z, Zhao-Peng Y, Zhi-Yong W (2003) Molecular chains: two new isomorphous coordination polymers of oxydiacetate. Inorg Chem Commun 6:706–709

Cortizo AM, Bruzzone L, Molinuevo MS, Etcheverry SB (2000) A possible role of oxidative stress in the vanadium-induced cytotoxicity in the MC3T3E1 osteoblast and UMR106 osteosarcoma cell lines. Toxicology 147:89–99

Cortizo MS, Alessandrini JL, Etcheverry SB, Cortizo AM (2001) A vanadium/aspirin complex controlled release using a poly(beta-propiolactone) film: effects on osteosarcoma cells. J Biomater Sci Polym 12:945–959

Costa Pessoa J, Cavaco I, Correia I, Tomaz AI, Adão P, Vale I, Ribeiro V, Castro MM, Geraldes CC (2007) Vanadium schiff base complexes: chemistry, properties, and concerns about possible therapeutic applications. In: Kustin K, Costa Pessoa J, Crans DC (eds) Vanadium: the versatile metal. ACS symposium series, vol 974. ACS, pp 340–351

Costas M, Mehn MP, Jensen L (2004) Dioxygen activation at mononuclear nonheme iron active sites: enzymes, models, and intermediates. Chem Rev 104:939–986

Crans DC (2000) Chemistry and insulin-like properties of vanadium(IV) and vanadium(V) compounds. J Inorg Biochem 80:123–131

Del Río D, Galindo A, Vicente R, Mealli C, Ienco A, Masi D (2003) Synthesis, molecular structure and properties of oxo vanadium(IV) complexes containing the oxydiacetate ligand. Dalton Trans 9:1813–1820

Dharwan S, Singh S, Aggarwal BB (1997) Induction of endothelial cell surface adhesion molecules by tumor necrosis factor is blocked by protein tyrosine phosphatase inhibitors: role of nuclear transcription factor NF-κB. Eur Immunol 27:2172–2179

Djordjevic C (1995) Antitumor activity of vanadium compounds. In: Sigel H, Sigel A (eds) Metal ions in biological systems, vol 31. Marcel Dekker, New York, pp 595–616

El-Naggara MM, El-Waseefa AM, El-Halafawyb KM, El-Sayed IH (1998) Antitumor activities of vanadium(IV), manganese(IV), iron(III), cobalt(II) and copper(II) complexes of 2-methylaminopyridine. Cancer Lett 33:71–76

Etcheverry SB, Cortizo AM (1998) Bioactivity of vanadium compounds on cells in culture. In: Nriagu JO (ed) Vanadium in the environment. Advances in environmental science and technology; part A (chap 15). Wiley, New York, pp 359–394

Etcheverry SB, Ferrer EG, Naso L, Barrio DA, Lezama L, Rojo T, Williams PAM (2007) Losartan and its interaction with copper(II): biological effects. Bioorg Med Chem 15:6418–6424

Evangelou AM (2002) Vanadium in cancer treatment. Crit Rev Oncol Hematol 42:249–265

Evangelou AM, Karkabounas S, Kalpouzos G, Malamas M, Liasko R, Stefanou D, Vlahos AT, Kabanos TA (1997) Comparison of the therapeutic effects of two vanadium complexes administered at low dose on benzo[a]pyrene-induced malignant tumors in rats. Cancer Lett 119:221–225

Farrell NP (1999) Chapter 1 "Overview" In: Farrell NP (ed) Uses of inorganic chemistry in medicine. The Royal Society of Chemistry, Cambridge, p 16

Fisher MB, Thompson SJ, Ribeiro V, Lechner MC, Rettie A (1998) P450-catalyzed in-chain desaturation of valproic acid: isoform selectivity and mechanism of formation of Delta 3-valproic acid generated by baculovirus-expressed CYP3A1. Arch Biochem Biophys 356:63–70

Fu Y, Wang Q, Yang XG, Yang XD, Wang K (2008) Vanadyl bisacetylacetonate induced G1/S cell cycle arrest via high-intensity ERK phosphorylation in HepG2 cells. J Biol Inorg Chem 13:1001–1009

Ghosh P, D'Cruz OJ, Narla RK, Uckun FM (2000) Apoptosis-inducing vanadocene compounds against human testicular cancer. Clin Cancer Res 6:1536–1545

Halliwell B, Gutteridge JMC (2007) Free radicals in biology and medicine. Oxford University Press, Oxford

Hanauske U, Hanauske AR, Marshall MH, Muggia VA, Von Hoff DD (1987) Biphasic effect of vanadium salts on in vitro tumor colony growth. Int J Cell Cloning 5:170–178

Harding MM, Moksdi G (2000) Antitumor metallocenes: structure-activity studies and interactions with biomolecules. Curr Med Chem 7:1289–1293

Harding MM, Harden GJ, Field LD (1993) A 31P NMR study of the interaction of the antitumor active metallocene Cp2MoCl2 with calf thymus DNA. FEBS Lett 322:291–294

Henderson L, Wolfreys A, Fedyk J, Bourner C, Windebank S (1998) The ability of the Comet assay to discriminate between genotoxins and cytotoxins. Mutagenesis 113:89–94

Hissin PJ, Hilf R (1996) A fluorometric method for determination of oxidized and reduced glutathione in tissues. Anal Biochem 74:214–226

Holko P, Ligeza J, Kisielewska J, Kordowiak AM, Klein A (2008) The effect of vanadyl sulphate ($VOSO_4$) on autocrine growth of human epithelial cancer cell lines. Pol J Pathol 59:3–8

Klein A, Holko P, Ligeza J, Kordowiak AM (2008) Sodium orthovanadate affects growth of some human epithelial cancer cells (A549, HTB44, DU145). Folia Biol (Krakow) 56:115–121

Kopf-Maier P, Wagner W, Kopf H (1981) In vitro cell growth inhibition by metallocene dichlorides. Cancer Chemother Pharmacol 5:237–241

Kostova I (2009) Titanium and vanadium complexes as anticancer agents. Anticancer Agents Med Chem 9:827–842

Liao W, McNutt MA, Zhu WG (2009) The comet assay: a sensitive method for detecting DNA damage in individual cells. Methods 48:46–53

Lippard SL, Berg JM (1984) Principles of bioinorganic chemistry. University Science Books, Mill Valley

Lloyd DR, Phillips DH, Carmichael PL (1997) Generation of putative intrastrand cross-links and strand breaks in DNA by transition metal ion-mediated oxygen radical attack. Chem Res Toxicol 10:393–400

Luber B, Candidus S, Handsbusch G, Mentele E, Hutzler P, Feller S, Voss J, Höfler H, Becker KF (2000) Tumor derived mutated E-cadherin influences beta-catenin

localization and increases susceptibility to actin cytoskeletal changes induced by pervanadate. Cell Adhes Commun 7:391–408

Majumder S, Dutta P, Mookerjee A, Choudhuri SK (2006) The role of a novel copper complex in overcoming doxorubicin resistance in Ehrlich ascites carcinoma cells in vivo. Chem Biol Interact 159:90–103

Molinuelo MS, Cortizo AM, Etcheverry SB (2008) Vanadium(IV) complexes inhibit adhesion, migration and colony formation of UMR106 osteosarcoma cells. Cancer Chemother Pharmacol 61:767–773

Molinuevo MS, Barrio DA, Cortizo AM, Etcheverry SB (2004) Antitumoral properties of two new vanadyl(IV) complexes in osteoblasts in culture: role of apoptosis and oxidative stress. Cancer Chemother Pharmacol 53:163–172

Mosmann T (1983) Rapid colorimetric assay for cellular growth and survival: application to proliferation and cytotoxicity assays. J Immunol Methods 65:55–63

Mueller S, Riedel HD, Stremmel W (1997) Determination of catalase activity at physiological hydrogen peroxide concentrations. Anal Biochem 245:55–60

Murray JH, Harding MM (1994) Organometallic anticancer agents: the effects of central metal and halide ligands on the interaction of metallocene dihalides Cp2MX2 with nucleic acid constituents. J Med Chem 37:1936–1941

Narla RK, Dong Y, Klis D, Uckun FM (2001) Bis(4,7-dimethyl-1,10-phenanthroline) sulfatooxovanadium(IV) as a novel antileukemic agent with matrix metalloproteinase inhibitory activity. Clin Cancer Res 7:1094–1101

Navara CS, Benyumov A, Vassilev A, Narla RK, Ghosh P, Uckun FM (2001) Vanadocenes as potent anti-proliferative agents disrupting mitotic spindle formation in cancer cells. Anticancer Drugs 12:369–376

Okajima T, Nakamura K, Zhang H, Ling N, Tanabe T, Yasuda T, Rosenfeld RG (1992) Sensitive colorimetric bioassays for insulin-like growth factor (IGF) stimulation of cell proliferation and glucose consumption: use in studies of IGF analogs. Endocrinology 130:2201–2212

Rivadeneira J, Barrio DA, Etcheverry SB, Baran EJ (2007) Spectroscopic characterization of a VO^{2+} complex of oxodiacetic acid and its bioactivity on osteoblast-like cells in culture. Biol Trace Elem Res 118:159–166

Rivadeneira J, Di Virgilio AL, Barrio DA, Muglia CI, Bruzzone L, Etcheverry SB (2010) Cytotoxicity of a vanadyl(IV) complex with a multidentate oxygen donor in osteoblast cell lines in culture. Med Chem 6:9–23

Rodríguez-Mercado JJ, Roldán-Reyes E, Altamirano-Lozano M (2003) Genotoxic effects of vanadium(IV) in human peripheral blood cells. Toxicol Lett 144:359–369

Rojas E, Valverde M, Herrera LA, Altamirano-Lozano M, Ostrosky-Wegman P (1996) Genotoxicity of vanadium pentoxide evaluated by the single cell gel electrophoresis in human lymphocytes. Mutat Res 359:77–84

Sakurai H (1994) Vanadium distribution in rats and DNA cleavage by vanadyl complex: implication for vanadium toxicity and biological effects. Environ Health Perspect 3:35–36

Sakurai H, Tamura H, Okatani K (1995) Mechanism for a new vanadium complex: hydroxyl radical-dependent DNA cleavage by 1,10-phenanthroline-vanadyl complex in the presence of hydrogen peroxide. Biochem Biophys Res Commun 206:133–137

Samanta S, Chatterjee M, Ghosh B, Rajkumar M, Rana A, Chatterjee M (2008) Vanadium and $1,25(OH)_2$ vitamin D3 combination in inhibitions of 1,2-dimethylhydrazine-induced rat colon carcinogenesis. Biochim Biophys Acta 1780:1106–1114

Singh NP, McCoy MT, Tice RR, Schneider EL (1988) A simple technique for quantitation of low levels of DNA damage in individual cells. Exp Cell Res 175:184–191

Sit KH, Paramananthan R, Bay B, Wong KP, Chan HL, Thong P, Watt E (1996) Sequestration of mitotic (M-phase) chromosomes in autophagosomes: mitotic programmed cell death in human Chang liver cells induced by an OH burst from vanadyl(IV). Anat Rec 245:1–8

Soares SS, Henao F, Aureliano M, Gutiérrez-Merino C (2008) Vanadote induces necrotic death in neonatal rat cardiomyocytes through mitochondrial membrane depolarization. Chem Res Toxicol 21:607–618

Toney JH, Brock CP, Marks TJ (1986) Aqueous coordination chemistry of vanadocene dichloride, with nucleotides and phosphoesters. Mechanistic implication for a new class of antitumor agents. J Am Chem Soc 108:7263–7274

Wozniak K, Blasiak J (2004) Vanadyl sulfate can differentially damage DNA in human lymphocytes and HeLa cells. Arch Toxicol 78:7–15

Yang XG, Yang XD, Yuan L, Wang K, Crans DC (2004) The permeability and cytotoxicity of insulin-mimetic vanadium compounds. Pharm Res 21:1026–1033

Younes M, Kayserb E, Strubelt O (1991) Effect of antioxidants on vanadate-induced toxicity towards isolated perfused rat livers. Toxicology 70:141–149